

## MAGNETIC FIELD STRUCTURE FROM SYNCHROTRON POLARIZATION

Rainer Beck<sup>1</sup>

**Abstract.** Total magnetic fields in spiral galaxies, as observed through their total synchrotron emission, are strongest (up to  $\simeq 30 \mu\text{G}$ ) in the spiral arms. The degree of radio polarization is low; the field in the arms must be mostly turbulent or tangled. Polarized synchrotron emission shows that the resolved *regular* fields are generally strongest in the interarm regions (up to  $\simeq 15 \mu\text{G}$ ), sometimes forming “magnetic arms” parallel to the optical arms. The field structure is spiral in almost every galaxy, even in flocculent and bright irregular types which lack spiral arms. The observed large-scale patterns of Faraday rotation in several massive spiral galaxies reveal coherent regular fields, as predicted by dynamo models. However, in most galaxies observed so far no simple patterns of Faraday rotation could be found. Either many dynamo modes are superimposed and cannot be resolved by present-day telescopes, or most of the apparently regular field is in fact *anisotropic random*, with frequent reversals, due to shearing and compressing gas flows. In galaxies with massive bars, the polarization pattern follows the gas flow. However, around strong shocks in bars, the compression of the regular field is much lower than that of the gas; the regular field decouples from the cold gas and is strong enough to affect the flow of the diffuse warm gas. – The average strength of the total magnetic field in the *Milky Way* is  $6 \mu\text{G}$  near the sun and increases to  $20\text{--}40 \mu\text{G}$  in the Galactic center region. The Galactic field is mostly parallel to the plane, except in the center region. Rotation measure data from pulsars indicate several field reversals, unlike external galaxies, but some reversals could be due to distortions of the nearby field.

### 1 The polarization foreground from the Milky Way

CMB experiments critically depend on the correction for emission from the Galactic foreground. Several surveys of the total Galactic radio emission and maps of

---

<sup>1</sup> MPI für Radioastronomie, Auf dem Hügel 69, 53121 Bonn, Germany

many selected fields exist (Reich et al. 2004b). The first absolutely calibrated all-sky polarization survey has just been completed at  $\lambda 21$  cm (1.4 GHz) (see Wolleben et al. 2006 for the northern part) which shows that polarized intensity has a much more complex structure than total intensity. It is not known yet which of the polarization structures, invisible in total emission, are real and which are due to wavelength- and latitude-dependent Faraday effects. The existing polarization data are insufficient to construct a realistic model. One of the “toy” models for CMB correction (Giardino et al. 2002) was based on an analysis of the angular power spectra of  $\lambda 13$  cm (2.4 GHz) polarization data in a region near the Galactic plane, with the (unrealistic) assumption that polarization angles have a random distribution. Furthermore, at  $\lambda 13$  cm Faraday effects are still strong in the Galactic plane. All-sky polarization surveys at higher frequencies are urgently needed, as well as better models of the magneto-ionic interstellar medium.

Another approach is to model the Galactic radio emission at high frequencies with help of models of the distribution of cosmic ray and magnetic fields in the Milky Way. However, testing the models is difficult. The available Galactic data from the radio and  $\gamma$  ranges and direct cosmic-ray detections are affected by the Local Bubble and other local structures. Radio observations of external spiral galaxies help to model the large-scale properties of regular and turbulent magnetic fields and cosmic rays.

## 2 Magnetic fields and synchrotron polarization observations

Learning about magnetic fields is not only important for Galactic models. Magnetic fields are a major agent in the interstellar medium (ISM). They contribute significantly to the total pressure which balances the ISM against gravitation. They may affect the gas flows in spiral arms and around bars. Magnetic fields are essential for the onset of star formation as they enable the removal of angular momentum from the protostellar cloud during its collapse. MHD turbulence distributes energy from supernova explosions within the ISM. Magnetic reconnection is a possible heating source for the ISM and halo gas. Magnetic fields also control the density and distribution of cosmic rays in the ISM.

*Polarized radio emission*, emitted by cosmic-ray electrons spiralling around magnetic fields in the interstellar or intergalactic medium, in pulsars and in background quasars, typically has a much higher degree of polarization than in the other spectral ranges. The observed degree of polarization is reduced by unpolarized thermal emission within the beam, which may dominate in star-forming regions, by *Faraday depolarization* (Sokoloff et al. 1998), and by geometrical depolarization due to variations of the field orientation within the beam.

The orientation of the polarization vectors is changed in a magneto-ionic medium by *Faraday rotation* which increases with  $\lambda^2$ . At small  $\lambda$  (below about 6 cm for typical ISM magnetic fields or about 1 cm for strong fields in starburst regions) the  $\mathbf{B}$ -vectors (i.e. the observed  $\mathbf{E}$ -vectors rotated by  $90^\circ$ ) trace, within a few degrees, the *orientation* of the field in the sky plane (Sect. 5). As  $\mathbf{B}$ -vectors are ambiguous by  $\pm 180^\circ$  and hence insensitive to field reversals, coherent regular and

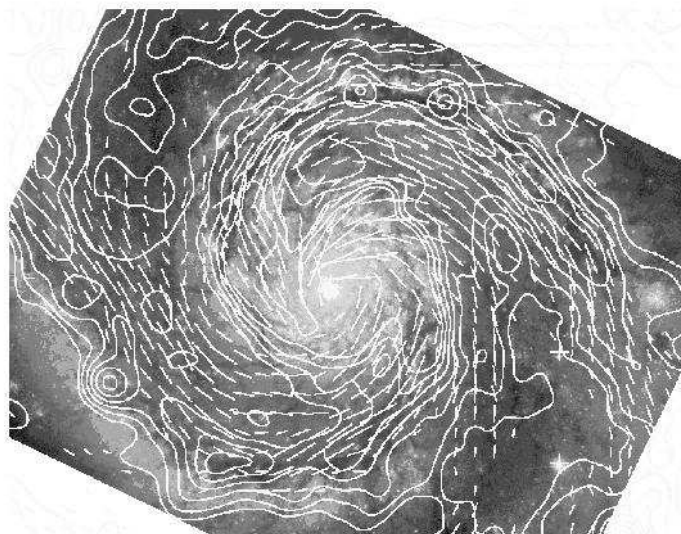


**Fig. 1.** Total radio intensity (contours) and  $\mathbf{B}$ -vectors of polarized intensity in the inner disk of the grand design spiral galaxy M 51 at  $6''$  resolution, combined from VLA and Effelsberg observations at  $\lambda 6$  cm. The field size is  $4' \times 3'$ . The length of the vectors is proportional to the polarized intensity. The background image shows the optical emission observed with the Hubble Space Telescope (Hubble Heritage Project) (from Fletcher et al. 2006).

anisotropic random (incoherent) fields cannot be distinguished. Coherent regular fields and their *direction* can be derived only from the strength and sign of Faraday rotation (Sect. 6).

### 3 Magnetic field strengths in galaxies

The average strength of the total  $\langle B_{t,\perp} \rangle$  and the resolved regular field (or anisotropic random field)  $\langle B_{\text{reg},\perp} \rangle$  in the plane of the sky can be derived from the total and polarized radio synchrotron intensity, respectively, if energy-density equipartition between cosmic rays and magnetic fields is assumed (Beck & Krause 2005).

The mean equipartition strength of the total field for a sample of 74 spiral galaxies is  $\langle B_t \rangle \simeq 9 \mu\text{G}$  (Niklas 1995). Radio-faint galaxies like M 31 and M 33 have  $\langle B_t \rangle \simeq 6 \mu\text{G}$ , while  $\simeq 15 \mu\text{G}$  is typical for grand-design galaxies like M 51, M 83 and NGC 6946. In the prominent spiral arms of M 51 the total field strength is  $\simeq 30 \mu\text{G}$  (Fletcher et al. 2004b), with peaks along the prominent dust lane (Fig. 1). The strongest fields in spiral galaxies were found in starburst galaxies, like M 82 with  $\simeq 50 \mu\text{G}$  strength (Klein et al. 1988) and the “Antennae” (Chyży & Beck 2004), and in nuclear starburst regions, like in NGC 1097 (Beck et al. 2005) and NGC 7552 with  $\simeq 100 \mu\text{G}$  strength (Beck et al. 2004). If energy losses

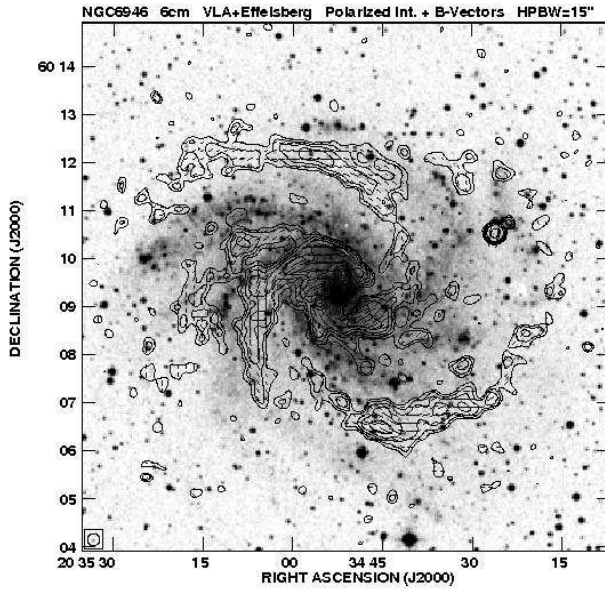


**Fig. 2.** Polarized radio intensity (contours) and  $\mathbf{B}$ -vectors of NGC 6946 at  $15''$  resolution, combined from VLA and Effelsberg observations at  $\lambda 6$  cm. The background grey-scale image shows the optical emission from the DSS (from Beck & Hoernes 1996)

of electrons are significant, these values are lower limits (Beck & Krause 2005).

The strengths of *regular* fields (or anisotropic random fields)  $B_{\text{reg}}$  in spiral galaxies (observed with a spatial resolution of a few 100 pc) are typically 1–5  $\mu\text{G}$ . Exceptionally strong regular fields are detected in the interarm regions of NGC 6946 of up to  $\simeq 13 \mu\text{G}$  (Beck & Hoernes 1996) and  $\simeq 15 \mu\text{G}$  at the inner edge of the inner spiral arms in M51 (Fletcher et al. 2004b). In the spiral arms of external galaxies the regular field is generally weak (Figs. 2 and Fig. 3), whereas the turbulent and unresolved tangled fields are strong due to turbulent gas motions and the expansion of supernova remnants. Dwarf irregular galaxies with almost chaotic rotation host turbulent fields with strengths comparable to spiral galaxies, but no detectable regular fields (Chyży et al. 2003).

#### 4 Magnetic energy densities

The relative importance of various competing forces in the interstellar medium can be estimated by comparing the corresponding energy densities. In the local Milky Way, the energy densities of turbulent gas motions, cosmic rays, and magnetic fields are similar (Boulares & Cox 1990). Global studies are possible in external galaxies (Beck 2004). In NGC 6946, the energy density of the magnetic field  $E_{\text{magn}}$  (assuming energy density equipartition with cosmic rays) is one order of magnitude

larger than that of the ionized gas  $E_{th}$  (assuming a volume filling factor of 5%). In the inner parts of NGC 6946, the energy densities of the total magnetic field and of turbulent gas motions are similar, but the field energy dominates in the outer parts due to the large radial scale length of the magnetic energy ( $\simeq 8$  kpc), compared to the scale length of about 3 kpc for the neutral gas density. If equipartition is no longer valid in the outer regions due to the lack of cosmic rays, the scale length of the magnetic field is even larger.

The energy density of global rotation of the neutral gas in the inner part of NGC 6946 is  $\simeq 500\times$  larger than that of the turbulent gas motion. As the radial decrease of magnetic energy density is much slower than that of the rotational energy density, the magnetic field energy density may reach the level of global rotational gas motion at some radius and hence affect the rotation curve, as proposed by Battaner & Florido (2000). However, this may only happen far out in a galaxy and is insufficient explain flat rotation curves.

In the outer parts of galaxies synchrotron emission cannot be detected, but the strengths of regular fields can still be measured by Faraday rotation of polarized background sources. Han et al. (1998) found evidence that the regular field in M31 extends to at least 25 kpc radius without significant decrease in strength. Hence we may consider that galaxies are surrounded by huge magnetic halos.

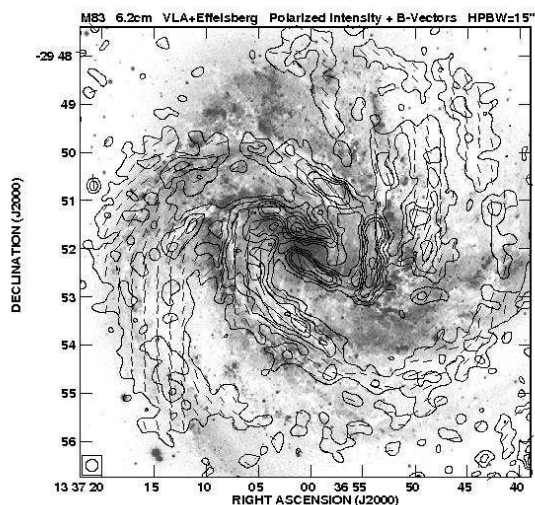


**Fig. 3.** Polarized radio intensity (contours) and  $\mathbf{B}$ -vectors of M 83 at  $15''$  resolution, combined from VLA and Effelsberg observations at  $\lambda 6$  cm (Beck, Ehle & Sukumar, unpublished). The background optical image is from the Anglo Australian Observatory (kindly provided by D. Malin)

## 5 Large-scale magnetic field structures in galaxies

Maps of the total radio emission and maps of the mid-infrared dust emission of external galaxies reveal a surprisingly close connection (Frick et al. 2001b, Vogler et al. 2005). The strongest total fields generally coincide with highest emission from dust and gas in the spiral arms (Fig. 1). This suggests a coupling of the tangled magnetic field to the warm dust mixed with the cool gas (Helou & Bicay 1993, Niklas & Beck 1997, Hoernes et al. 1998).

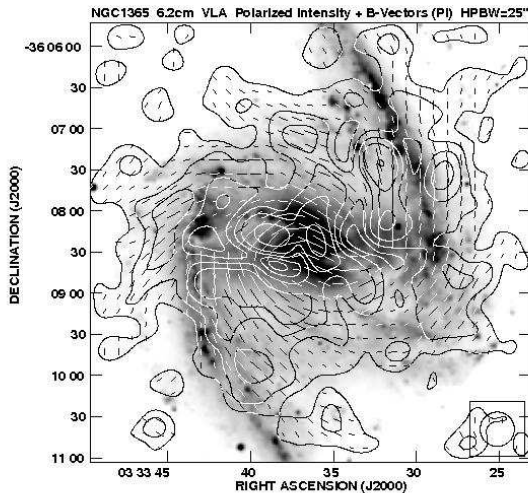


**Fig. 4.** Polarized radio intensity (contours) and  $\mathbf{B}$ -vectors of the barred galaxy NGC 1365 at  $25''$  resolution from VLA observations at  $\lambda 6$  cm. The grey-scale image shows an optical emission from the ESO observatory (kindly provided by P.O. Lindblad) (from Beck et al. 2005).

The  $\mathbf{B}$ -vectors of polarized emission form spiral patterns, not only in spiral galaxies, but also in flocculent and several bright irregular galaxies (see examples shown in Beck 2005). The magnetic field runs almost parallel to the spiral arms. In M 51, the field orientation varies by  $10^\circ$ – $20^\circ$  around the pitch angles of the spiral arms as traced by CO emission (Patrikeev et al. 2006). In galaxies with strong density waves, like M 51, the regular field fills the whole interarm space, but is strongest at the positions of the dust lanes on the inner edge of the spiral arms (Fletcher et al. 2004b, Fig. 1). In most other galaxies, the polarized emission is strongest *between* the optical arms, sometimes forming *magnetic spiral arms* with ridge lines between the optical arms (like in NGC 6946, Fig. 2, and in M 83, Fig. 3) or across the arms, like in NGC 3627 (Soida et al. 2001).

In strongly barred galaxies, gas and stars move in highly noncircular orbits. Numerical models show that gas streamlines are deflected in the bar region along shock fronts, behind which the gas is compressed in a fast shearing flow. M83

(Fig. 3) hosts a small bar, NGC 1097 and NGC 1365 (Fig. 4) host huge bars. The total radio intensity is strongest in the region of the dust lanes, consistent with compression by the bar’s shock. The polarized intensity in NGC 1097 and NGC 1365 (Fig. 4) has a completely different distribution. The  $\mathbf{B}$ -vectors and the gas streamlines around the bar as obtained in numerical simulations are surprisingly similar, which suggests that the regular magnetic field is generally aligned with the shearing flow (Beck et al. 1999a). Remarkably, the optical images of NGC 1097 and NGC 1365 show dust filaments which are almost perpendicular to the bar and aligned with the  $\mathbf{B}$ -vectors. However, the upstream/downstream contrast in polarized intensity is significantly smaller than that expected from compression and shearing of the regular magnetic field, which could be the result of decoupling of the regular field from the dense molecular clouds (Beck et al. 2005). The regular field in the bar is probably strong enough to resist shearing by the rarefied diffuse gas. These observations, for the first time, indicate that *magnetic forces can control the flow of the diffuse interstellar gas at kiloparsec scales*.

Present-day polarization observations are limited by sensitivity at high resolution. The best available spatial resolutions are 100–300 pc in the nearest spiral galaxies and 10 pc in the LMC (Gaensler et al. 2005). Data on beam and Faraday depolarization in NGC 6946 (Beck et al. 1999b), assuming single-sized cells, indicate that the interstellar field is tangled on scales of  $\simeq 20$  pc. The EVLA and the planned Square Kilometre Array (SKA) will have much improved sensitivities. The SKA will allow to study magnetic field structures in nearby galaxies at angular resolutions more than  $10\times$  better than today (Beck & Gaensler 2004).

## 6 Spiral fields: coherent or anisotropic?

Dynamo action generates *coherent* spiral magnetic fields, while compression or shearing of turbulent fields by gas flows generates *incoherent anisotropic random* fields, which reverse direction frequently within the telescope beam, so that Faraday rotation is small while the degree of polarization can still be high. (Note that polarization angles are insensitive to field reversals.) Only Faraday rotation is a signature of coherent regular fields, and the sense of Faraday rotation reveals the direction of the field. Large-scale (“mean field”) galactic dynamo models generate spiral fields with large-scale coherence. Observation of large-scale patterns in Faraday rotation shows that a significant fraction of the field has a coherent direction and has been generated by a large-scale dynamo.

The large-scale field structure obtained in  $\alpha$ - $\Omega$  dynamo models is described by modes of different azimuthal, radial, and vertical symmetries (Beck et al. 1996). Several modes can be excited. In flat disks with axisymmetric gas distribution and smooth rotation, the strongest mode is the axisymmetric spiral one ( $m = 0$ ) with even vertical symmetry (quadrupole), followed by the weaker  $m = 1$  (a bisymmetric spiral field), etc. These modes can be identified by Fourier analysis of their specific azimuthal RM patterns (Krause 1990).

Real galaxies are not uniform. Consequently, recent dynamo models include the non-axisymmetric gas distribution in spiral arms (Moss 1998) or the gas flow

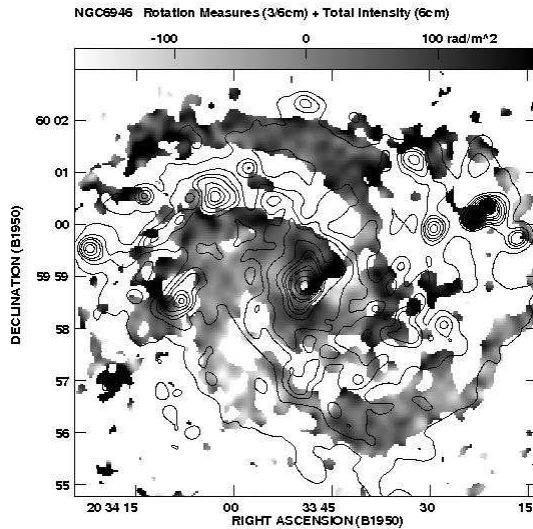


**Fig. 5.** Grey-scale map of the Faraday rotation measures of NGC 6946 between  $\lambda 3$  cm and  $\lambda 6$  cm at  $15''$  resolution, overlaid onto contours of total intensity at  $\lambda 6$  cm. The data were obtained from combined polarization observations with the VLA and Effelsberg telescopes (Beck, unpublished).

in a bar potential (Moss et al. 2001) where higher modes may be amplified faster than in the standard model. Gravitational interaction with another galaxy may also modify the mode spectrum and enhance the bisymmetric mode (Moss 1995).

M 31 hosts a strongly dominating axisymmetric field (Berkhuijsen et al. 2003), extending to at least 25 kpc radius (Han et al. 1998) and at least 1 kpc height above the galaxy's plane (Fletcher et al. 2004a). Other candidates for a dominating axisymmetric field are IC 342 (Krause et al. 1989a) and the LMC (Gaensler et al. 2005). A bisymmetric mode dominates in M 81 (Krause et al. 1989b).

*Magnetic arms* (Sect. 5) may evolve between the optical arms if the dynamo number is smaller in the gaseous arms than between them, e.g. due to increased turbulent velocity of the gas in the arms (Moss 1998, Shukurov 1998) or if magnetic turbulent diffusion is larger in the arms. The magnetic arms in NGC 6946 can be described as a superposition of an axisymmetric  $m = 0$  and a quadrisymmetric  $m = 2$  mode (Rohde et al. 1999). The RMs are preferably positive in the northern and negative in the southern half of the galaxy (Fig. 5). However, RM fluctuations on a scale of about 1 kpc are superimposed onto the large-scale coherent field, and the amplitude of the fluctuations is larger than that of the coherent field.

The massive spiral M 51 is of special interest: While previous low-resolution data indicated a mixture of axisymmetric and bisymmetric fields in the disk and a dominating axisymmetric field in the halo (Berkhuijsen et al. 1997), recent observations with higher resolution show that Faraday rotation fluctuates on small



scales with amplitudes much larger than those of the large-scale modes (Fletcher et al. 2006). This means that the anisotropic random field is stronger than the coherent regular field, possibly due to shearing and compressing in a strong density wave flow.

Several other spiral galaxies revealed a highly ordered spiral pattern in the polarization ( $\mathbf{B}-$ ) vectors, but small Faraday rotation, so that anisotropic random fields seem to dominate over the coherent regular ones. In the barred galaxies NGC 1097 and NGC 1365 (Fig. 4) the high degrees of polarization along the bar are mostly due to compressed random fields (Beck et al. 2005). Ram pressure from the intracluster gas or interaction between galaxies have a similar compressional effect, e.g. in the “Antennae” (Chyży & Beck 2004).

For most of about 20 nearby galaxies for which RM data are available, no dominating magnetic modes could be reliably determined (Beck 2000). Either these galaxies host a mixture of dynamo modes which cannot be resolved due to the large telescope beam and/or to the low signal-to-noise ratio. The Square Kilometre Array (SKA) will dramatically improve the quality of polarization data (Beck & Gaensler 2004) and allow detailed tests of galactic dynamo models (Beck 2006).

## 7 Magnetic field strength and large-scale structure in the Milky Way

The strength of the total field  $\langle B_t \rangle$  is  $6 \mu\text{G}$  near the Sun and about  $10 \mu\text{G}$  in the inner Galaxy (Berkhuijsen, in Beck 2001), assuming equipartition between the energy densities of magnetic fields and cosmic rays. In our Galaxy the accuracy of the equipartition assumption can be tested, because we have independent information about the local cosmic-ray energy density from in-situ measurements and about their radial distribution from  $\gamma$ -ray data. Combination with the radio synchrotron data yields a local strength of the total field  $\langle B_t \rangle$  of  $6 \mu\text{G}$  (Strong et al. 2000), the same value as derived from energy equipartition. The radial scale length of the equipartition field of  $\simeq 12 \text{ kpc}$  is also similar to that in Strong et al. (2000). In the nonthermal filaments near the Galactic center the field strength may reach several  $100 \mu\text{G}$  (Reich 1994, Yusef-Zadeh et al. 1996), but the pervasive diffuse field is much weaker (Novak 2004), probably  $20\text{--}40 \mu\text{G}$  (LaRosa et al. 2005, scaled for a proton/electron ratio of 100).

Synchrotron polarization observations in the local Galaxy imply a ratio of regular to total field strengths of  $\langle B_{\text{reg}}/B_t \rangle \simeq 0.6$  (Berkhuijsen 1971, Brouw & Spoelstra 1976, Heiles 1996). The total radio emission along the local spiral arm requires that  $\langle B_{\text{reg}}/B_t \rangle = 0.6\text{--}0.7$  (Phillipps et al. 1981). For  $\langle B_t \rangle = 6 \pm 2 \mu\text{G}$  these results give  $4 \pm 1 \mu\text{G}$  for the local regular field component (including anisotropic random fields).

Rotation measure and dispersion measure data of pulsars give an average strength of the local coherent regular field of  $\langle B_{\text{reg}} \rangle = 1.4 \pm 0.2 \mu\text{G}$  (Rand & Lyne 1994, Han & Qiao 1994, Indrani & Deshpande 1998). In the inner Norma arm, the average strength of the coherent regular field is  $4.4 \pm 0.9 \mu\text{G}$  (Han et al. 2002). Han et al. (2006) claim that the regular field is stronger in the Galac-

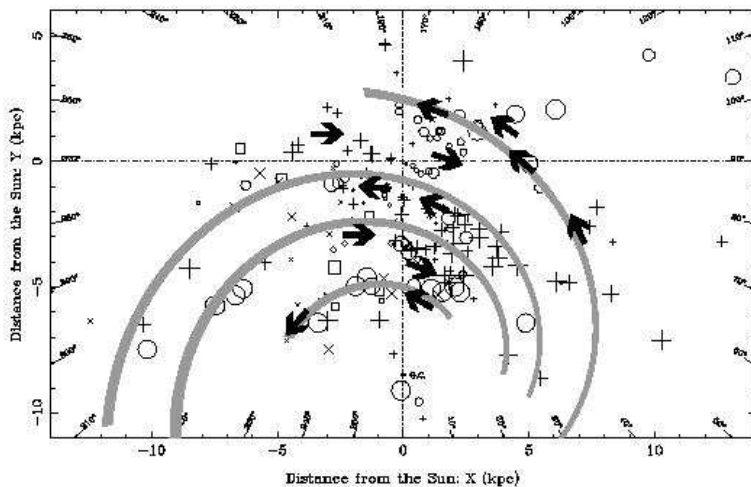


**Fig. 6.** Bird's eye view of the distribution of the RMs of pulsars within  $8^\circ$  of the Galactic plane. Positive RMs are shown as crosses and X, negative RMs as circles and open squares. The symbol sizes are proportional to the square root of  $|RM|$ , with the limits of 5 and  $250 \text{ rad/m}^2$ . The directions of the bisymmetric field model are given as arrows. The approximate location of four optical spiral arms is indicated as dotted lines (from Han et al. 1999a).

tic arms than in interarm regions, in contrast to the results in external galaxies (Sect. 3). The values for  $\langle B_{\text{reg}} \rangle$  derived from pulsar data are smaller than the equipartition estimates. The former are underestimates if small-scale fluctuations in field strength and in electron density are anticorrelated, as expected for local pressure equilibrium (Beck et al. 2003). On the other hand, the equipartition values for  $\langle B_{\text{reg}} \rangle$  derived from polarized intensities overestimate the strength of the coherent regular field if anisotropic turbulent fields (see Sect. 6) are present.

The local Galactic field is oriented mainly parallel to the plane, with only a weak vertical component of  $B_z \simeq 0.2 \mu\text{G}$  (Han & Qiao 1994). Fig. 6 shows the location of pulsars with measured RMs within the Galactic plane and the derived directions of the large-scale field (Han et al. 1999a). The Sun is located between two spiral arms, the Sagittarius/Carina and the Perseus arms. The mean pitch angle of the spiral arms is  $\simeq -18^\circ$  for the stars and  $-13^\circ \pm 1^\circ$  for all gas components (Vallée 1995, 2002). Starlight polarization and pulsar RM data (Fig. 6) give a significantly smaller pitch angle ( $-8^\circ \pm 1^\circ$ ) for the local magnetic field (Heiles 1996, Han & Qiao 1994, Indrani & Deshpande 1998, Han et al. 1999a). The local field may form a *magnetic arm* located between two optical arms. Differences between the pitch angles of the field and of the adjacent spiral arms of  $10^\circ$ – $20^\circ$  were also found in the spiral galaxy M 51 (Patrikeev et al. 2006).

## 8 Magnetic field reversals in the Milky Way

A puzzling property of the Galactic magnetic field is the existence of several *reversals* along Galactic radius, derived from pulsar RM data (Rand & Lyne 1994, Vallée 1995, Han et al. 1999a, Frick et al. 2001a). To account for these reversals, an axisymmetric field with radial reversals (Vallée 1996) or a *bisymmetric* magnetic spiral with a small pitch angle have been proposed (Han & Qiao 1994, Indrani & Deshpande 1998, Han et al. 2002, Fig. 6). Han et al. (2006) even claim that the interarm field is directed opposite to that in the arms.

It is striking that only very few field reversals have been detected in external spiral galaxies. High-resolution maps of Faraday rotation, which measure the RMs of the diffuse polarized synchrotron emission, are available for a couple of spiral galaxies. A dominating bisymmetric field structure was found only in M 81 (Krause et al. 1989), but the pitch angle is large and only two azimuthal reversals occur on opposite sides of the disk. The disk fields of M 51 and NGC 4414 can be described by a mixture of dynamo modes (Berkhuijsen et al. 1997, Soida et al. 2002), which appears as one single radial reversal to an observer located within the disk (Shukurov 2005). In NGC 2997, a radial field reversal between the disk and the central region occurs at about 2 kpc radius (Han et al. 1999b). However, no multiple reversals along radius, like those in the Milky Way, were found so far in any external galaxy.

The discrepancy between Galactic and extragalactic data may be due to the different observational methods. RMs in external galaxies are averages over the line of sight through the whole disk and halo and over the large telescope beam, and they may miss field reversals if these are restricted to a thin disk near the galaxy plane. The results in the Milky Way are based on RMs of pulsars, which trace the warm magneto-ionic medium near the plane along narrow lines of sight. Some of the Galactic reversals may not be of Galactic extent, but due to local field distortions or loops of the anisotropic turbulent field. Pulsar RMs around a star formation complex indeed revealed a field distortion which may mimic the reversal claimed to exist in the direction of the Perseus arm (Mitra et al. 2003). More RM data from Galactic pulsars are needed to obtain a clearer picture of the large-scale field structure. The SKA will detect about 20000 pulsars and obtain RMs from most of these (Cordes et al. 2004).

Further indication that the structure of the local Galactic magnetic field is rather complicated on pc and sub-pc scales comes from RM maps obtained from the diffuse Galactic synchrotron on which many reversals on small scales observed around 330 MHz with the WSRT (Haverkorn et al. 2003a, 2003b). Major progress can be expected from the new 1.4 GHz International Galactic Plane Survey observed at the DRAO and ATCA telescopes (Brown & Taylor 2001, Haverkorn et al. 2006, Brown et al. 2006). It will provide high-resolution RM data of the diffuse emission and several 100 RM values of polarized background sources. Preliminary results of average extragalactic RMs (Fig. 7) show a smooth large-scale structure on scales of tens of degrees, obviously caused by regular magnetic fields along the spiral arms. However, this appears to be different from the results for

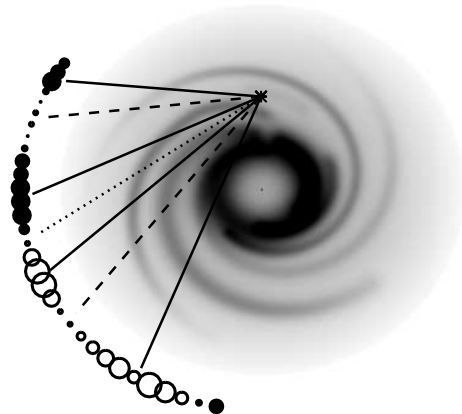


**Fig. 7.** Bird's eye view of the Galaxy, where the grey scale denotes the electron density model by Cordes & Lazio (2003) and circles represent RMs of extragalactic sources, binned over  $9^\circ$  in Galactic longitude. Open (closed) circles are negative (positive) RMs, and the largest circle denotes  $\text{RM} = -484 \text{ rad m}^{-2}$ . The solid lines are  $|\text{RM}|$  maxima, the dashed lines are  $|\text{RM}|$  minima, and the dotted line denotes a large-scale sign change in RM (from Brown et al. 2006).

external galaxies where the largest  $|\text{RM}|$  are found in interarm regions (Sect. 3). RMs in Fig. 7 are generally positive for Galactic longitudes smaller than  $300^\circ$  and negative at larger longitudes, different from what one would expect from pulsar RMs (Fig. 6). The decrease of  $|\text{RM}|$  to almost zero (dashed and dotted lines) can only occur if there are large-scale magnetic field reversals along the line of sight, although not necessarily on Galactic scales.

Fig. 5 may help to explain some of the apparent discrepancies between RM data from external galaxies and those in the Milky Way. An observer inside NGC 6946 would detect the RM pattern of the weak coherent field only for sufficiently long pathlengths (though along *interarm* regions). At distances below a few kpc, the fluctuations in RM with frequent reversals dominate. We need a realistic model of the field to predict what an internal observer would see, given a limited number of pathlengths to pulsars or background sources.

## 9 Small-scale field structures in the Milky Way

Present-day polarization observations of external galaxies are restricted to angular resolutions of  $5''$ – $10''$  because at higher resolutions polarized intensities are too low. Before much more sensitive telescopes like the SKA become operational, the small-scale structure of interstellar magnetic fields has to be investigated by polarization

observations in the Milky Way.

The Galactic magnetic field has a significant turbulent component with a mean strength of  $\simeq 5 \mu\text{G}$  (Rand & Kulkarni 1989, Ohno & Shibata 1993). Magnetic turbulence occurs over a large spectrum of scales, with the largest scale determined from pulsar RMs of  $l_{\text{turb}} \simeq 55 \text{ pc}$  (Rand & Kulkarni 1989) or  $l_{\text{turb}} \simeq 10 - 100 \text{ pc}$  (Ohno & Shibata 1993). These values are consistent with  $l_{\text{turb}} \simeq 20 \text{ pc}$  derived from depolarization data in the galaxy NGC 6946 (Beck et al. 1999b). In a test region in the southern Galactic plane, Haverkorn et al. (2004b) determined the structure function of RM fluctuations which reveals an outer scale of about 2 pc, possibly induced by HII regions.



**Fig. 8.** Polarized intensity around the plane of the Milky Way ( $l = 150^\circ - 174^\circ$ ,  $b = -4.5^\circ - +4.5^\circ$ ) at 1.4 GHz ( $\lambda 21 \text{ cm}$ ), combined from Effelsberg and Dwingeloo data (from Reich et al. 2004a).

Major progress in detecting small structures has been achieved with decimeter-wave observations of diffuse polarized emission from the Milky Way with the Effelsberg, ATCA, DRAO, and WSRT telescopes (Junkes et al. 1987, Duncan et al. 1997, 1999, Uyaniker et al. 1998, 1999, 2003, Gaensler et al. 2001, Uyaniker & Landecker 2002, Haverkorn et al. 2003a, 2003b, 2004a, Kothes & Landecker 2004, Reich et al. 2004a). A wealth of structures on pc and sub-pc scales has been discovered: filaments, canals, lenses, and rings (Fig. 8). Their common property is to appear only in the maps of polarized intensity, but not in total intensity. The interpretation is hampered by several difficulties. Firstly, large-scale emission in Stokes parameters Q and U is missing in interferometric and even in single-dish maps so that the polarized intensities and angles can be distorted severely (Reich et al. 2004a). Secondly, the wavelengths of these polarization surveys are rather long, so that strong depolarization of background emission in the foreground Faraday screen may lead to apparent structures like *Faraday ghosts* (Shukurov & Berkhuijsen 2003). On the other hand, such features carry valuable information about the turbulent ISM in the Faraday screen.

Another effect of Faraday depolarization is that, especially at decimeter wavelengths, only emission from nearby regions may be detected. The ISM is not

always transparent for polarized radio waves, and the opacity varies strongly with wavelength and position. The wavelength dependence of Faraday depolarization allows *Faraday tomography* of different layers if maps at different (nearby) wavelengths are combined (applying the method of *RM synthesis* by Brentjens & de Bruyn 2005).

A Galactic 5 GHz polarization survey, which should be mostly free of Faraday effects, has been started with the Urumqi telescope (Han & Reich, in prep.).

## 10 Magnetic fields in halos of galaxies and the Milky Way

Most edge-on galaxies possess thick radio disks of 1–3 kpc scale height (Lisenfeld et al. 2004) with magnetic field orientations mainly parallel to the disk (Dumke et al. 1995). A prominent exception is NGC 4631 with the brightest and largest halo observed so far, composed of vertical magnetic spurs connected to star-forming regions in the disk (Golla & Hummel 1994). NGC 5775 is an intermediate case with parallel and vertical field components (Tüllmann et al. 2000, Fig. 9), similar to the Milky Way (see below).

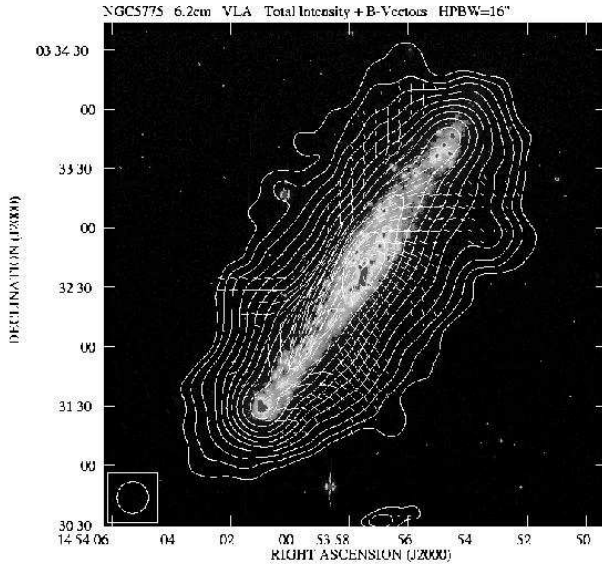


**Fig. 9.** Total radio intensity (contours) and  $\mathbf{B}$ -vectors of NGC 5775 at  $16''$  resolution, observed with the VLA at  $\lambda 6$  cm (from Tüllmann et al. 2000).

The vertical full equivalent thickness of the thick radio disk of the Milky Way is  $\simeq 3$  kpc near the Sun (Beuermann et al. 1985, scaled to a distance to the Galactic center of 8.5 kpc), corresponding to an exponential scale height of  $h_{\text{syn}} \simeq 1.5$  kpc. In case of equipartition between the energy densities of magnetic field and cosmic rays, the scale height of the total field is  $\simeq 4$  times larger than that of

the synchrotron disk,  $h_{B_t} \simeq 6$  kpc.  $h_{B_t}$  may be larger if cosmic rays originate from star-forming regions in the plane and are not re-accelerated in the halo, so that the electrons lose their energy above some height and the equipartition formula yields too small values for the field strength (Beck & Krause 2005).

Dynamo models predict the preferred generation of quadrupole fields where the toroidal component (traced by RMs) has the same sign above and below the plane. In external galaxies, no RM data of sufficient quality are presently available. In the Milky Way, RMs of extragalactic sources (see Han, in Wielebinski 2005, for a recent compilation) and RMs of pulsars reveal that no large-scale reversal exists near the plane for Galactic longitudes  $l = 90^\circ - 270^\circ$ . Thus the local field is part of a large-scale symmetric (quadrupole) field structure parallel to the Galactic plane. Towards the inner Galaxy ( $l = 270^\circ - 90^\circ$ ) the signs are opposite above and below the plane. This may indicate a global antisymmetric (dipole) mode (Han et al. 1997, Men & Han 2003) with a poloidal field component perpendicular to the plane, but an effect of local structures cannot be excluded. Remarkably, submm polarization observations indicate a poloidal magnetic field in low-density clouds in the vicinity of the Galactic center (Chuss et al. 2003).

## 11 Concluding remarks

Understanding and modelling the diffuse polarized emission from the Milky Way needs major efforts from both the observational and theoretical sides. At low frequencies, polarization data are of limited use for CMB studies because they are seriously affected by Faraday effects. These, on the other hand, have the potential to reveal new information on the structure and composition of the magnetized interstellar medium. For CMB studies and modelling, mapping the Galaxy in polarization at high frequencies is required. However, a polarization survey can only be reliably interpreted if missing large-scale structures in Stokes Q and U, e.g. by missing short spacings of synthesis telescopes, are corrected. External galaxies are useful for modelling the distribution of cosmic rays and the strength and large-scale structure of interstellar magnetic fields. Results which are apparently unique for the Milky Way, like frequent large-scale magnetic field reversals and large  $|\text{RM}|$  along spiral arms, should be taken with caution and further investigated with better data.

## References

- Battaner, E., & Florido, E. 2000, *Fund. Cosmic Phys.*, 21, 1
- Beck, R. 2000, *Phil. Trans. R. Soc. Lond. A*, 358, 777
- Beck, R. 2001, *Space Science Reviews*, 99, 243
- Beck, R. 2004, in *How Does the Galaxy Work?*, eds. E.J. Alfaro et al. (Dordrecht: Kluwer), p. 277
- Beck, R. 2005, in *Cosmic Magnetic Fields*, eds. R. Wielebinski & R. Beck (Berlin: Springer), p. 41
- Beck, R. 2006, *AN*, 327, 512

- Beck, R., & Hoernes, P. 1996, *Nature*, 379, 47
- Beck, R., & Gaensler, B.M. 2004, in *Science with the Square Kilometer Array*, eds. C. Carilli & S. Rawlings (Amsterdam: Elsevier), *New Astronomy Rev.*, 48, 1289
- Beck, R., & Krause, M. 2005, *AN*, 326, 414
- Beck, R., Brandenburg, A., Moss, D., Shukurov, A., & Sokoloff, D. 1996, *ARA&A*, 34, 155
- Beck, R., Ehle, M., Shoutenkov, V., Shukurov, A., & Sokoloff, D. 1999a, *Nature*, 397, 324
- Beck, R., Berkhuijsen, E. M., & Uyaniker, B. 1999b, in: *Plasma Turbulence and Energetic Particles in Astrophysics*, eds. M. Ostrowski & R. Schlickeiser (Kraków: Jagiellonian Univ.), p. 5
- Beck, R., Shukurov, A., Sokoloff, D., & Wielebinski, R. 2003, *A&A*, 411, 99
- Beck, R., Ehle, M., Fletcher, A., et al. 2004, in *The Evolution of Starbursts*, eds. S. Hüttemeister et al., *AIP Conf. Proc.*, 783, p. 216
- Beck, R., Fletcher, A., Shukurov, A., et al. 2005, *A&A*, 444, 739
- Berkhuijsen, E.M. 1971, *A&A*, 14, 359
- Berkhuijsen, E.M., Horellou, C., Krause, M., Neining, N., Poezd, A.D., Shukurov, A., & Sokoloff, D.D. 1997, *A&A*, 318, 700
- Berkhuijsen, E.M., Beck, R., & Hoernes, P. 2003, *A&A*, 398, 937
- Beuermann, K., Kanbach, G., & Berkhuijsen, E. M. 1985, *A&A*, 153, 17
- Boulares, A., & Cox, D.P. 1990, *ApJ*, 365, 544
- Brentjens, M. A., & de Bruyn, A. G. 2005, *A&A*, 441, 1217
- Brouw, W.N., & Spoelstra, T. A. Th. 1976, *A&AS*, 26, 129
- Brown, J. C., & Taylor, A. R. 2001, *ApJ*, 563, L31
- Brown, J. C., et al. 2006, in prep.
- Chuss, D. T., Davidson, J. A., Dotson, J. L., et al. 2003, *ApJ*, 599, 1116
- Chyży, K. T., & Beck, R. 2004, *A&A*, 417, 541
- Chyży, K. T., Beck, R., Kohle, S., et al. 2000, *A&A*, 356, 757
- Chyży, K. T., Knapik, J., Bomans, D. J., Klein, U., Beck, R., Soida, M., & Urbanik, M. 2003, *A&A*, 405, 513
- Cordes, J.M., & Lazio, T. J. W. 2003, astro-ph/0301598
- Cordes, J.M., Kramer, M., Lazio, T. J. W., Stappers, B. W., Backer, D.C., & Johnston, S. 2004, in *Science with the Square Kilometer Array*, eds. C. Carilli & S. Rawlings (Amsterdam: Elsevier), *New Astronomy Rev.*, 48, 1413
- Dumke, M., Krause, M., Wielebinski, R., & Klein, U. 1995, *A&A*, 302, 691
- Duncan, A. R., Haynes, R. F., Jones, K. L., & Stewart, R. T. 1997, *MNRAS*, 291, 279
- Duncan, A. R., Reich, P., Reich, W., & Fürst, E. 1999, *A&A*, 350, 447
- Ehle, M., Pietsch, W., Beck, R., & Klein, U. 1998, *A&A*, 329, 39
- Fletcher, A., Berkhuijsen, E. M., Beck, R., & Shukurov, A. 2004a, *A&A*, 414, 53
- Fletcher, A., Beck, R., Berkhuijsen, E. M., Horellou, C., & Shukurov, A. 2004b, in *How Does the Galaxy Work?*, eds. E. J. Alfaro et al. (Dordrecht: Kluwer), p. 299
- Fletcher, A., Beck, R., Berkhuijsen, E. M., Horellou, C., & Shukurov, A. 2006, in prep.
- Frick, P., Stepanov, R., Shukurov, A., & Sokoloff, D. 2001a, *MNRAS*, 325, 649
- Frick, P., Beck, R., Berkhuijsen, E. M., & Patrickeyev, I. 2001b, *MNRAS*, 327, 1145



- Gaensler, B. M., Dickey, J. M., McClure-Griffiths, N. M., et al. 2001, *ApJ*, 549, 959
- Gaensler, B. M., Haverkorn, M., Staveley-Smith, L., et al. 2005, *Science*, 307, 1610
- Giardino, G., Banday, A. J., Górski, K. M., Bennett, K., Jonas, J. L., & Tauber, J. 2002, *A&A*, 387, 82
- Golla, G., & Hummel, E. 1994, *A&A*, 284, 777
- Han, J. L., & Qiao, G. J. 1994, *A&A*, 288, 759
- Han, J. L., Manchester, R. N., Berkhuijsen, E. M., & Beck, R. 1997, *A&A*, 322, 98
- Han, J. L., Beck, R., & Berkhuijsen, E. M. 1998, *A&A*, 335, 1117
- Han, J. L., Manchester, R. N., & Qiao, G. J. 1999a, *MNRAS*, 306, 371
- Han, J. L., Beck, R., Ehle, M., Haynes, R. F., & Wielebinski, R. 1999b, *A&A*, 348, 405
- Han, J. L., Manchester, R. N., Lyne, A. G., & Qiao, G. J. 2002, *ApJ*, 570, L17
- Han, J. L., Manchester, R. N., Lyne, A. G., Qiao, G. J., & van Straten, W. 2006, *ApJ*, 642, 868
- Haverkorn, M., Katgert, P., & de Bruyn, A. G. 2003a, *A&A*, 403, 1031
- Haverkorn, M., Katgert, P., & de Bruyn, A. G. 2003b, *A&A*, 404, 233
- Haverkorn, M., Katgert, P., & de Bruyn, A. G. 2004a, *A&A*, 427, 549
- Haverkorn, M., Gaensler, B. M., Brown, J. C., McClure-Griffiths, N. M., Dickey, J. D., & Green, A. J. 2004b, *ApJ*, 609, 776
- Haverkorn, M., Gaensler, B. M., Brown, J. C., McClure-Griffiths, N. M., Dickey, J. D., & Green, A. J. 2006, *AN*, 327, 483
- Heiles, C. 1996, in *Polarimetry of the Interstellar Medium*, eds. W. G. Roberge & D. C. B. Whittet, ASP Conf. Ser., 97, p. 457
- Helou, G., & Bica, M. D. 1993, *ApJ*, 415, 93
- Hoernes, P., Berkhuijsen, E. M., & Xu, C. 1998, *A&A*, 334, 57
- Indrani, C., & Deshpande, A. A. 1998, *New Astronomy*, 4, 33
- Junkes, N., Fürst, E., & Reich, W. 1987, *A&AS*, 69, 451
- Klein, U., Wielebinski, R., & Morsi, H. W. 1988, *A&A*, 190, 41
- Kothes, R., & Landecker, T. L. 2004, in *The Magnetized Interstellar Medium*, eds. B. Uyaniker et al. (Copernicus: Katlenburg), p. 33
- Krause, M. 1990, in *Galactic and Intergalactic Magnetic Fields*, eds. R. Beck et al. (Dordrecht: Kluwer), p. 187
- Krause, M., Hummel, E., & Beck, R. 1989a, *A&A*, 217, 4
- Krause, M., Beck, R., & Hummel, E. 1989b, *A&A*, 217, 17
- LaRosa, T. N., Brogan, C. L., Shore, S. N., Lazio, T. J., Kassim, N. E., & Nord, M. E. 2005, *ApJ*, 626, L23
- Lisenfeld, U., Dahlem, M., & Ehle, M. 2004, in *How Does the Galaxy Work?*, eds. E. J. Alfaro et al. (Dordrecht: Kluwer), p. 75
- Men, H., & Han, J. L. 2003, *Act. Astr. Sinica*, 44, 151
- Mitra, D., Wielebinski, R., Kramer, M., & Jessner, A. 2003, *A&A*, 398, 993
- Moss, D. 1995, *MNRAS*, 275, 191
- Moss, D. 1998, *MNRAS*, 297, 860
- Moss, D., Shukurov, A., Sokoloff, D., Beck, R., & Fletcher, A. 2001, *A&A*, 380, 55
- Niklas, S. 1995, PhD Thesis, University of Bonn

- Niklas, S., & Beck, R. 1997, *A&A*, 320, 54
- Novak, G. 2004, in *Magnetic Fields in the Universe*, eds. E. M. de Gouveia Dal Pino et al., AIP Conf. Proc., 784, p. 329
- Ohno, H., & Shibata, S. 1993, *MNRAS*, 262, 953
- Patrikeev, I., Fletcher, A., Stepanov, R., Beck, R., Berkhuijsen, E. M., Frick, P., & Horellou, C. 2006, *A&A*, in press
- Phillipps, S., Kearsy, S., Osborne, J. L., Haslam, C. G. T., & Stoffel, H. 1981, *A&A*, 103, 405
- Rand, R. J., & Kulkarni, S. R. 1989, *ApJ*, 343, 760
- Rand, R. J., & Lyne, A. G. 1994, *MNRAS*, 268, 497
- Reich, W. 1994, in *The Nuclei of Normal Galaxies*, eds. R. Genzel & A. I. Harris (Dordrecht: Kluwer), p. 55
- Reich, W., Fürst, E., Reich, P., Uyaniker, B., Wielebinski, R., & Wolleben, M. 2004a, in *The Magnetized Interstellar Medium*, eds. B. Uyaniker et al. (Copernicus: Katlenburg), p. 45
- Reich, P., Reich, W., & Testori, J. C. 2004b, in *The Magnetized Interstellar Medium*, eds. B. Uyaniker et al. (Copernicus: Katlenburg), p. 63
- Rohde, R., Beck, R., & Elstner, D. 1999, *A&A*, 350, 423
- Shukurov, A. 1998, *MNRAS* 299, L21
- Shukurov, A. 2005, in *Cosmic Magnetic Fields*, eds. R. Wielebinski & R. Beck (Berlin: Springer), p. 113
- Shukurov, A., & Berkhuijsen, E. M. 2003, *MNRAS*, 342, 496
- Soida, M., Urbanik, M., Beck, R., Wielebinski, R., & Balkowski, C. 2001, *A&A*, 378, 40
- Soida, M., Beck, R., Urbanik, M., & Braine, J. 2002, *A&A*, 394, 47
- Sokoloff, D. D., Bykov, A. A., Shukurov, A., Berkhuijsen, E. M., Beck, R., & Poezd, A. D. 1998, *MNRAS*, 299, 189, and *MNRAS*, 303, 207 (Erratum)
- Strong, A. W., Moskalenko, I. V., & Reimer, O. 2000, *ApJ*, 537, 763
- Tüllmann, R., Dettmar, R.-J., Soida, M., Urbanik, M., & Rossa, J. 2000, *A&A*, 364, L36
- Uyaniker, B., & Landecker, T. L. 2002, *ApJ*, 575, 225
- Uyaniker, B., Fürst, E., Reich, W., Reich, P., & Wielebinski, R. 1998, *A&AS*, 132, 401
- Uyaniker, B., Fürst, E., Reich, W., Reich, P., & Wielebinski, R. 1999, *A&AS*, 138, 31
- Uyaniker, B., Landecker, T. L., Gray A. D., & Kothes, R. 2003, *ApJ*, 585, 785
- Vallée, J. P. 1995, *ApJ*, 454, 119
- Vallée, J. P. 1996, *A&A*, 308, 433
- Vallée, J. P. 2002, *ApJ*, 566, 261
- Vogler, A., Madden, S. C., Beck, R., et al. 2005, *A&A*, 441, 491
- Wielebinski, R. 2005, in *Cosmic Magnetic Fields*, eds. R. Wielebinski & R. Beck (Berlin: Springer), p. 89
- Wolleben, M., Landecker, T. L., Reich, W., & Wielebinski, R. 2006, *A&A*, 448, 411
- Yusef-Zadeh, F., Roberts, D. A., Goss, W. M., Frail, D. A., & Green, A. J. 1996, *ApJ*, 466, L25